PNAS RESEARCH ARTICLE | GENETICS

The neurotrophic factor MANF regulates autophagy and lysosome function to promote proteostasis in *Caenorhabditis elegans*

Shane K. B. Taylor[a], Jessica H. Hartman[b,c], and Bhagwati P. Gupta[a,1]

Affiliations are included on p. 12.

Edited by Andrew Dillin, University of California, Berkeley, CA; received February 24, 2024; accepted August 29, 2024 by Editorial Board Member Ulrich Hartl

The conserved mesencephalic astrocyte-derived neurotrophic factor (MANF) is known for protecting dopaminergic neurons and functioning in various other tissues. Previously, we showed that *Caenorhabditis elegans manf-1* null mutants exhibit defects such as increased endoplasmic reticulum (ER) stress, dopaminergic neurodegeneration, and abnormal protein aggregation. These findings suggest an essential role for MANF in cellular processes. However, the mechanisms by which intracellular and extracellular MANF regulate broader cellular functions remain unclear. We report a unique mechanism of action for MANF-1 that involves the transcription factor HLH-30/TFEB-mediated signaling to regulate autophagy and lysosomal function. Multiple transgenic strains overexpressing MANF-1 showed extended lifespan of animals, reduced protein aggregation, and improved neuronal survival. Using fluorescently tagged MANF-1, we observed tissue-specific localization of the protein, which was dependent on the ER retention signal. Further subcellular analysis showed that MANF-1 localizes within cells to the lysosomes and utilizes the endosomal pathway. Consistent with the lysosomal localization, our transcriptomic study of MANF-1 and analyses of autophagy regulators demonstrated that MANF-1 promotes proteostasis by regulating autophagic flux and lysosomal activity. Collectively, our findings establish MANF as a critical regulator of stress response, proteostasis, and aging.

nematode | MANF-1 | ER stress | longevity | proteostasis

Significance

Dysregulation of protein homeostasis can lead to harmful protein aggregation, a hallmark of age-related diseases. The neurotrophic factor, mesencephalic astrocyte-derived neurotrophic factor (MANF), protects cells from such protein aggregates and promotes survival of neurons. Given MANF's therapeutic promise, understanding its molecular mechanism is vital. Our study demonstrates a unique role for MANF in autophagy and lysosome function, critical processes for clearing toxic proteins. In the animal model *Caenorhabditis elegans*, overexpressing MANF extended lifespan, reduced protein clumps, and conferred protection on neurons. These roles of MANF are mediated by the HLH-30/TFEB, a master regulator of lysosome function. Our findings demonstrate MANF's critical role in maintaining cellular equilibrium, offering unique insights into its potential applications in combating age-associated disorders.

Cellular homeostasis requires a delicate balance of protein synthesis and degradation, and specialized machinery to ensure that proteins fold properly and identify misfolded or damaged proteins. However, the ability of cells to maintain protein homeostasis declines with age (1). Dysregulated homeostasis can cause protein misfolding and the formation of protein aggregates. Accumulation of these aggregates increases cellular stress, disrupts physiological processes, and eventually results in the failure of cells, tissues, and organs. Maintaining protein homeostasis (proteostasis) is essential for proper cellular function, reducing age-related diseases, and promoting healthy aging (1–3). Notably, cells can activate stress response signaling pathways, such as the unfolded protein response (UPR), to maintain proteostasis and minimize cellular damage. Although these responses are highly efficient in clearing protein aggregates, their functional capacity diminishes with age. Failure to eliminate toxic protein aggregates is a key hallmark of age-related diseases, including neurodegenerative disorders like Parkinson's Disease (PD) and Huntington's Disease (HD) (1, 4, 5).

A promising approach to proteostasis and protecting against neurodegeneration involves the therapeutic delivery of neurotrophic factors (NTFs). NTFs are proteins that support neuronal survival, growth, and differentiation. Their anti-inflammatory and antiapoptotic properties make them promising therapeutic candidates (6). One family of NTFs relevant to this study includes the cerebral dopamine neurotrophic factor (CDNF) and the mesencephalic astrocyte-derived neurotrophic factor (MANF) (7). These two proteins are structurally and mechanistically distinct from other classical NTFs (6, 8). Although vertebrates express both CDNF and MANF, a single ortholog is expressed in invertebrates and it which closely resembles MANF (9, 10).

MANF homologs have been studied in various animals, including the vertebrates mouse, rat, zebrafish, and the invertebrates *Drosophila melanogaster* and *Caenorhabditis elegans* (9, 11–14). These studies have shown that MANF confers cytoprotection through the regulation of the endoplasmic reticulum (ER)-UPR (7). The ER-UPR is a quality control mechanism that rectifies cellular stress by correctly folding misfolded proteins,

The authors declare no competing interest.

This article is a PNAS Direct Submission A.D. is a guest editor invited by the Editorial Board.

[1]To whom correspondence may be addressed. Email: guptab@mcmaster.ca.

This article contains supporting information online at https://www.pnas.org/lookup/suppl/doi:10.1073/pnas.2403906121/-/DCSupplemental.

Published October 17, 2024.

reducing translation, and activating apoptosis when homeostasis cannot be restored (15). Three conserved transmembrane proteins mediate the ER-UPR, inositol-requiring enzyme 1 (IRE1), protein kinase RNA (PKR)-like ER kinase (PERK), and activating transcription factor 6 (ATF6) (*ire-1*, *pek-1*, and *atf-6*, respectively, in *C. elegans*), which activate overlapping but distinct pathways in stress responses (15, 16). Additionally, IRE1 creates a spliced form of the transcription factor X-box binding protein-1 (XBP1), the main regulator of ER-UPR. Spliced XBP-1 maintains homeostasis through the transcription of chaperones, such as GRP78/BiP (*C. elegans hsp-4*), which is affected by MANF (2, 15–18). Consistent with the role of MANF in ER-UPR maintenance, its sequence contains an ER retention signal (19). Under normal conditions, MANF is retained in the ER and is secreted in response to protein misfolding or cellular stress (20). However, it remains to be investigated how MANF elicits its protective benefits once at target tissues and cells.

Recent studies have indicated that MANF is also linked to other diseases with dysregulated homeostasis, more specifically, metabolic dysfunction, diabetes, ischemia, and retinal degeneration (6, 21, 22). Accordingly, MANF is widely expressed (21–24) underscoring the protein's critical roles in multiple tissues and processes, despite its designation as a NTF. Although MANF is secreted from the ER in response to stress, the mechanism by which it regulates cellular function and how extracellular MANF affects other tissues, organelles, and processes remain unclear. Additionally, whether there is a common theme underlying its mechanisms of action in different cell types is not known. Studies on the *C. elegans* MANF homolog, MANF-1, have shown that it is secreted and endocytosed upon binding to sulfatides (25). Our group and others have demonstrated the role of MANF-1 in processes that include age-dependent protection of dopaminergic (DA) neurons (9), regulation of the ER-UPR chaperone HSP-4/BIP/GRP78, and sensitivity to bacterial pathogenesis (10, 26). The protective role of *manf-1* may involve its interaction with genes that mediate autophagy, ER-UPR, and immunity (10, 26).

This study reports unique findings on MANF-1's requirements and its mechanism of action. Our data showed that *manf-1* mutants died prematurely when subjected to ER stress and that MANF-1 expression was up-regulated in response to stress-inducing conditions. Further analysis revealed an essential role for this gene in regulating ER-UPR signaling. We generated multiple transgenic strains overexpressing MANF-1 (both MANF-1 alone and MANF-1::mCherry chimera) and found that the animals had longer lifespans, improved proteostasis, and reduced neurodegeneration. Additionally, the MANF-1::mCherry animals had broad expression in areas including the intestine, pharynx, muscles, hypodermis, and coelomocytes. Subcellular analysis revealed that MANF-1 was secreted and localized to lysosomal membranes. Further characterization of MANF-1::mCherry showed variations in expression pattern depending on the presence or absence of the ER retention signal; however, the lysosomal localization remained consistent in the transgenic strains carrying different *manf-1* constructs. Moreover, the MANF-1 expression pattern was broadly similar in animals carrying either the *C. elegans* ER sequence (KEEL) or the human version (RTDL). Interestingly, the beneficial effects of MANF-1 overexpression did not depend on the ER sequence.

Consistent with the role of MANF-1 in the ER and lysosomes, transcriptomic profiling of the mutant and overexpressing animals revealed significant changes in the expression of ER-UPR and lysosomal genes. We found that MANF-1 secretion and subcellular localization required endosomal trafficking proteins such as RAB-5 and RAB-7. Further experiments investigating autophagy using LGG-1 and p62/SQST-1 reporters suggest that MANF-1 regulates autophagic flux. Additionally, MANF-1 overexpression caused HLH-30/TFEB, a transcription factor that regulates autophagy and lysosomal biogenesis, to be up-regulated and localized to the nucleus. The protective benefits of MANF were found to be mediated by HLH-30/TFEB. Altogether, our findings establish MANF-1 as more than a neurotrophic factor, but rather as a key player in regulating ER-UPR, autophagy, and lysosomal function, potentially in a coordinated manner to promote proteostasis, neuroprotection, and the lifespan of animals.

Results

***manf-1* Mutants Show Increased ER Stress Sensitivity and a Shorter Lifespan.** We previously reported that *manf-1* mutants exhibit increased expression of the ER-UPR reporter *hsp-4p::GFP* and are resistant to tunicamycin-induced growth delay, during larval exposures (9, 10). Given that the ER-UPR function declines with age (1, 27) we aimed to explore the age-dependent effects of elevated ER stress on these mutants. Specifically, we evaluated the impact of *manf-1* loss in older *manf-1(tm3603)* adults by administering the ER stress-activating agent tunicamycin. Analysis of *hsp-4p::GFP* fluorescence in 1-, 4-, and 7-d-old animals revealed significantly higher levels in *manf-1(tm3603)* mutants compared to controls (Fig. 1 *A* and *B*). The *hsp-4* transcription upregulation was also confirmed by qPCR (Fig. 1 *C* and *D*). These findings underscore the essential role of *manf-1* in maintaining ER-UPR across both young and older adults. Our experiments also demonstrated that *manf-1(tm3603)* mutants have a significantly reduced lifespan (Fig. 1*E*; mean and max lifespans for this and subsequent experiments are in Dataset S1). Tunicamycin treatment exacerbated the DA neurodegeneration, lifespan reduction, and mortality in these animals (Fig. 1 *F* and *G* and *SI Appendix*, Fig. S1*A*).

Consistent with the above results, *manf-1p::GFP* fluorescence was significantly increased following tunicamycin treatment (Fig. 1*H*). Similarly, *manf-1* transcription was up-regulated in animals subjected to both acute (8 h) and chronic (3 d) exposures (Fig. 1 *I* and *J*). The endogenously tagged *mKate2::manf-1* strain (10) exhibited a similar upregulation of MANF-1 in response to tunicamycin, demonstrating that an increase in mRNA led to an increase in protein (Fig. 1*K*).

We also examined whether *manf-1* influences the sensitivity of animals to other forms of stress, aiming to understand the gene's role in various physiological processes. To this end, we performed heat stress and oxidative stress assays. Except for paraquat, where chronic exposure resulted in significant damage to DA neurons in *manf-1* mutants (*SI Appendix*, Fig. S1*B*), no notable differences were observed between mutant and wild-type animals (*SI Appendix*, Fig. S1 *C* and *D*). Collectively, the results presented in this section demonstrate that *manf-1* is essential for maintaining ER-UPR and protecting animals against ER stress.

***manf-1* Mutants Show Enhanced Protein Aggregation Defects.** Based on the upregulation of *hsp-4* in *manf-1(tm3603)* animals, we investigated the ER-UPR genes that define each of the signaling arms, namely ATF6/*atf-6*, PERK/*pek-1*, IRE1/*ire-1*, and the downstream transcription factor XBP-1/*xbp-1* (2, 15). The expression of all four genes was significantly up-regulated in *manf-1* mutants compared to wild-type controls (Fig. 2*A*). The ratio of spliced to total *xbp-1* was also high (Fig. 2*B*). These data suggest that *manf-1* affects a wide range of processes that maintain ER homeostasis.

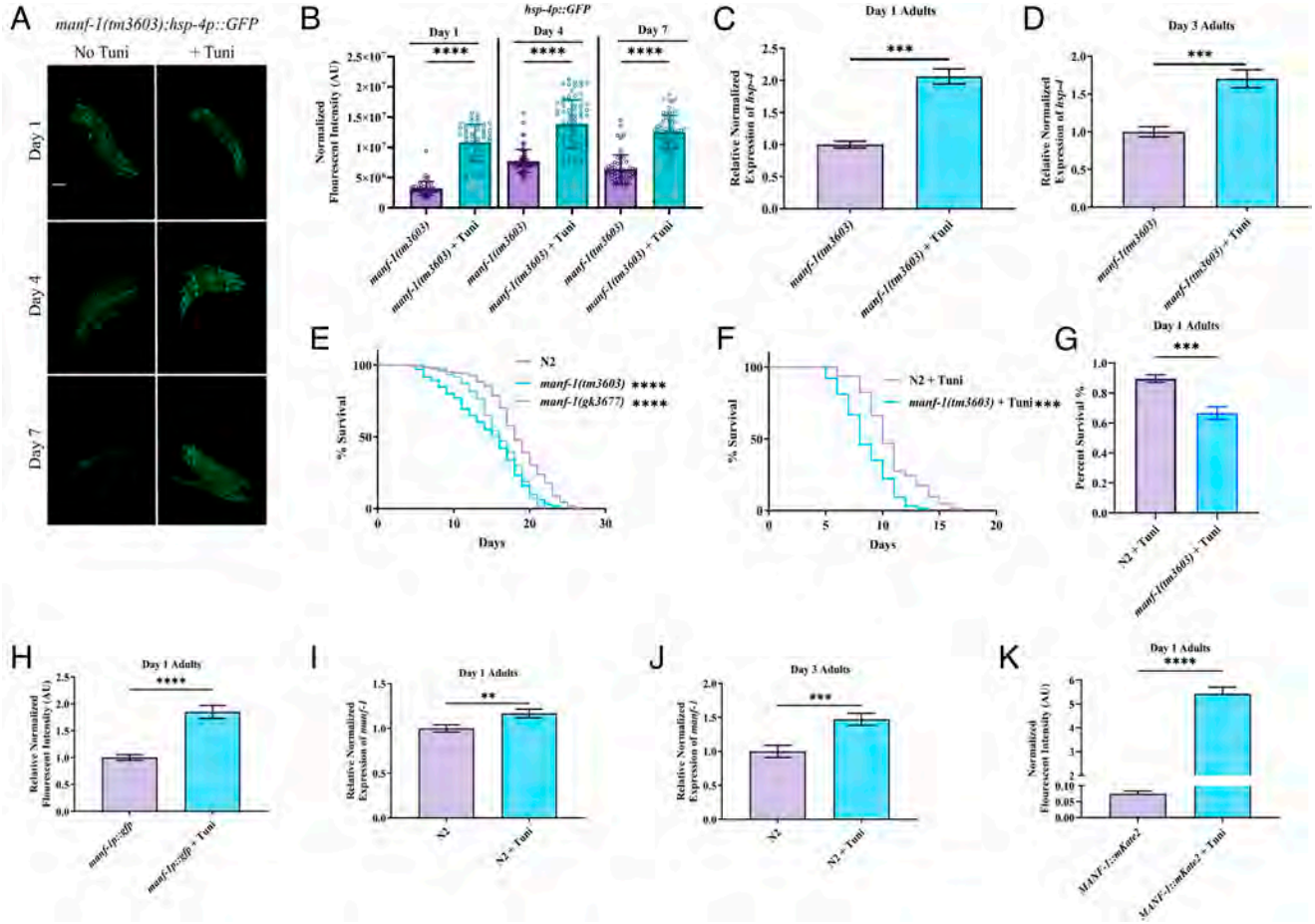

Fig. 1. *manf-1* mutants show increased ER-UPR, and *manf-1* expression is up-regulated following ER stress. (*A*) Representative images of *manf-1(tm3603)*; *hsp-4p::GFP* animals with and without 4 h of 25 ng/μL tunicamycin exposure on days 1, 4, and 7 of adulthood. (Scale bar, 100 μm.) (*B*) Fluorescence intensity plot of corresponding animals. (*C*) RT-qPCR of *hsp-4* in day 1 *manf-1(tm3603)* adults following 8 h exposure to 5 μg/mL tunicamycin. (*D*) Same as *C*, except that animals were chronically exposed to 5 μg/mL tunicamycin until day 3 of adulthood. (*E* and *F*) Lifespan analysis of *manf-1* mutants and N2 control (*E*) and following chronic exposure to 25 ng/μL tunicamycin (*F*). Mean and max lifespan are in Dataset S1. (*G*) Percentage survival following 4 h exposure to 50 ng/μL tunicamycin in liquid. (*H*) GFP fluorescence quantification in *manf-1p::GFP* day 1 adults following 8 h of 5 μg/mL tunicamycin treatment. (*I*) *manf*-1 RT-qPCR in day 1 N2 adults following 8 h of 5 μg/mL tunicamycin treatment. (*J*) Same as *I*, except that animals were chronically exposed to 5 μg/mL tunicamycin until day 3 of adulthood. (*K*) mKate2 fluorescence quantification in the *manf-1p::mKate2::manf-1* transgenic strain. For results in *A*, *E–H*, and *K*, 60 to 140 total worms from three batches (20 worms minimum per batch) were examined. The RT-qPCR experiments (*C*, *D*, *I*, and *J*) were carried out in three batches. The graphs are plotted as mean ± SEM (*C*, *D*, *G*, and *H–K*) and mean ± SD (*B*). Data were analyzed using Student's *t* test (*B–D* and *G–K*) and the log-rank (Kaplan–Meier) method (*E* and *F*). **P* < 0.05; ***P* < 0.01; ****P* < 0.001; *****P* < 0.0001.

As ER stress reduces the ability of cells to promote protein folding and causes the accumulation of misfolded and unfolded proteins, we examined the proteostasis defects in *manf-1* mutants. To this end, transgenic animals expressing YFP reporter-tagged human α-Synuclein in body wall muscles were used. In a previous study, we demonstrated that these transgenic animals showed increased aggregation in the absence of *manf-1* (9). Analysis of α-Synuclein::YFP in 1-, 4-, and 7-d-old *manf-1 (tm3603)* adults revealed higher fluorescence compared to wild-type controls (Fig. 2*C*), suggesting that *manf-1* is necessary to maintain proteostasis at different stages of adulthood. The animals also showed increased protein aggregation and slower rates of thrashing (Fig. 2 *D* and *E*). The aggregation phenotype was further enhanced by RNAi knockdown of *atf-6* and *pek-1* (*SI Appendix*, Fig. S2 *A–D*), providing support for the conclusion that ER-UPR was compromised but not eliminated in the absence of *manf-1*. In contrast, the *manf-1(tm3603); xbp-1*(RNAi) animals showed an opposite effect, with significantly reduced α-Synuclein::YFP levels (*SI Appendix*, Fig. S2 *A–D*). Although the precise reasons are unknown, we noted that despite the apparent protection from protein aggregation, the *manf-1(tm3603); xbp-1* (RNAi) animals were unhealthy and exhibited slower growth, abnormal movement, reduced viability, and a tendency to frequently burst open through the vulval opening (see *Materials and Methods* and *SI Appendix*, Fig. S3). These observations suggest that *xbp-1* knockdown significantly compromised physiological processes in *manf-1* mutants, leading to reduced α-Synuclein aggregation. The synthetic interaction between *manf-1* and *xbp-1* was consistent with previous findings that reported that *manf-1; ire-1* double mutants and *xbp-1* RNAi-treated *manf-1* mutants were lethal or sterile (10).

Next, we investigated the effect of *manf-1* mutation on α-Synuclein-induced DA neurodegeneration. To this end, a strain expressing *α-Synuclein* under the *dat-1* promoter (dopamine transporter) was utilized. Examination of day 7 *manf-1(tm3603); dat-1p::a-Synuclein* adults showed increased neurodegeneration (*SI Appendix*, Fig. S4). The result further supports the essential role of MANF-1 in proteostasis and survival of neurons.

We used another protein aggregation system to examine the effects of *manf-1*, which consists of glutamine repeats (polyQ) and serves as a *C. elegans* HD model (28). To this end, two polyQ strains (AM140 Q35::YFP and AM141 Q40::YFP) that express fusion proteins in body wall muscles under the *unc-54* promoter were utilized (28). Similar to α-Synuclein, both polyQ strains exhibited

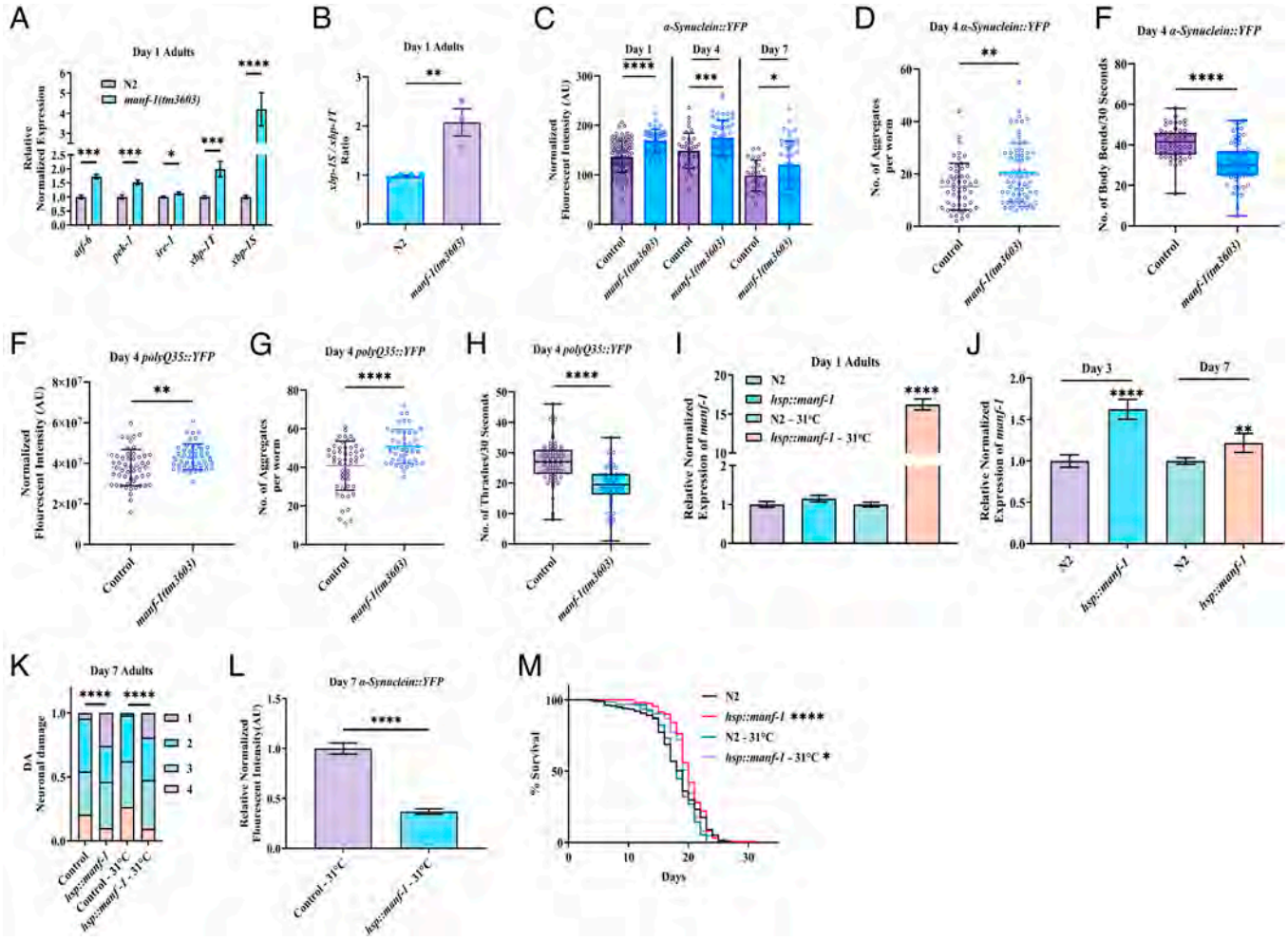

Fig. 2. *manf-1* mutants show protein aggregation defects, and *hsp::manf-1* is neuroprotective and extends lifespan. (*A*) RT-qPCR of ER-UPR genes (*atf-6, pek-1, ire-1,* and *xbp-1)* in N2 and *manf-1(tm3603)* day 1 adults. *xbp-1* total and spliced forms are indicated by *xbp-1T* and *xbp-1S*, respectively. (*B*) The ratio of spliced *xbp-1* to total *xbp-1* in *manf-1(tm3603)* day 1 adults. (*C*) Fluorescence intensity of α-Synuclein::YFP in body wall muscles measured in day 1, 4, and 7 adults. (*D*) α-Synuclein::YFP aggregation phenotype in day 4 adults. (*E*) Thrashing response of α-Synuclein::YFP in *manf-1(tm3603)* animals over a 30-s interval compared to control. (*F–H*) polyQ35 aggregation phenotype in *manf-1(tm3603)* animals on day 4 of adulthood compared to wild-type. The total fluorescent intensity of polyQ35::YFP (*F*) and number of aggregates (*G*) in body wall muscles. The thrashing response over a 30-s interval (*H*). (*I*) RT-qPCR of *manf-1* expression in day 1 *hsp::manf-1* and N2 adults maintained either at 20 °C or subjected to 1 h heat shock at 31 °C. (*J*) RT-qPCR of day 3 and day 7 adults grown at 20 °C. (*K*) Neuronal analysis in day 7 *hsp::manf-1* and control adults. An odd-day heat treatment at 31 °C starting on day 1 until day 7 was used. See *Materials and Methods* for neuron scoring (1, normal cell bodies and dendrites; 2, dendritic damage; 3, cell body missing or abnormally shaped; and 4, both dendrites and cell bodies defective). (*L*) Effect of MANF-1 overexpression on α-Synuclein aggregation. Fluorescent intensity of α-Synuclein::YFP in day 7 adults following the same heat treatment as in *K*. (*M*) Lifespan following heat treatments as in *K*. Mean and max lifespan are in Dataset S1. Results in *A* and *B* are based on three batches of pooled worms. For *C–H*, at least three batches were analyzed (10 to 20 worms per batch). Data in panels *I–K* include three different batches. For α-Synuclein and lifespan analyses, three batches with 20 to 30 animals per batch were examined. Results are shown as mean ± SEM (*A*, *B*, *I*, *J*, and *L*) and mean ± SD (*C–G*). Panel *H* shows a box plot containing all data points, mean, and 25th and 75th quartile boundaries. Data were analyzed using Student's *t* test (*A–H* and *L*), one-way ANOVA with Tukey's test (*I* and *J*), Chi-squared test (*K*), and log-rank (Kaplan–Meier) method (*M*). *$P < 0.05$; **$P < 0.01$; ***$P < 0.001$; ****$P < 0.0001$. ns: not significant.

a significant increase in protein aggregation in *manf-1* mutants (Fig. 2 *F* and *G* and *SI Appendix*, Fig. S2 *E* and *F*). Thrashing defects in the polyQ35 animals, due to aggregates accumulating in muscles, were also enhanced (Fig. 2*H*). One possibility is that the observed increase in aggregates was an artifact of higher levels of the polyQ and α-Synuclein proteins in the genetically altered strains. Therefore, we performed western blotting experiment. The results revealed no significant changes in either protein in *manf-1(tm3603)* animals compared to the controls (*SI Appendix*, Fig. S5). Thus, we conclude that *manf-1* is necessary for regulating ER-UPR signaling and preventing protein aggregation.

Overexpression of *manf-1* Reduces Protein Aggregation, Improves Neuronal Survival, and Extends Lifespan. The essential role of *manf-1* in stress response maintenance and proteostasis suggests that overexpression of this gene might have protective and beneficial effects. To test this hypothesis, we employed various approaches to activate *manf-1* expression. One approach involved treating animals with bioactive compounds such as curcumin and lithium, which have been reported to increase *manf* transcription in mammalian cells (29, 30). Similar experiments in worms also showed increased *manf-1* levels, albeit modestly. Other methods involved the use of transgenic strains expressing *manf-1* under the control of either the heat-shock *hsp-16.41* promoter (*hsp::manf-1*) or the native promoter (*manf-1p::manf-1* and *manf-1p::manf-1::mCherry*; see *Materials and Methods*).

For the *hsp::manf-1* strain, we tested whether inducing *manf-1* expression had a cytoprotective effect in animals. The transgenic worms exhibited a robust response to heat treatment, as a 1-h exposure to 31 °C significantly increased *manf-1* transcription (Fig. 2*I*). Notably, heat shock was not required at later stages since 3- and 7-d-old adults showed significant expression without treatment (Fig. 2*J*), likely due to basal promoter activity at room temperature.

Phenotypic analysis of 7-d-old *hsp::manf-1; dat-1p::YFP* adults revealed increased protection of DA neurons following heat treatment. Specifically, these animals had a higher proportion of morphologically normal dendritic processes and cell bodies (Fig. 2*K*). Quantification of neuronal defects showed fewer animals with defective dendritic and cell body morphologies, demonstrating *manf-1*'s role in promoting the survival of neurons. Interestingly, animals without heat treatment also exhibited comparable neuroprotection (Fig. 2*K*), suggesting that a mild increase in MANF-1 levels is sufficient to protect DA neurons. Additionally, the *hsp::manf-1* transgene resulted in significantly lower YFP fluorescence in *hsp::manf-1; α-Synuclein::YFP* animals, indicating reduced protein aggregation in older adults (Fig. 2*L*). Finally, lifespan was significantly extended (approximately 5% in heat-treated animals and 23% in untreated animals; Fig. 2*M*).

Next, we examined the phenotype of *manf-1p::MANF-1::mCherry* transgenic animals (termed *MANF-1*$^{KEEL::mCherry}$; see *Materials and Methods*). The *MANF-1*$^{KEEL::mCherry}$ worms showed high levels of secreted MANF-1 across three different lines examined (see next section and *Materials and Methods*). One of these lines, showing high transgene transmission (DY759, *bhEx304*), was analyzed in detail. While *hsp-4* transcripts were not significantly affected in these animals, the *hsp-4p::GFP* analysis showed increased fluorescence (Fig. 3 *A* and *B* and *SI Appendix*, Fig. S6). Thus, *manf-1* overexpression caused a modest activation of ER-UPR. We also observed an increase in both total and spliced *xbp-1* transcripts, whereas *pek-1* levels were reduced (*SI Appendix*, Fig. S6). However, *MANF-1*$^{KEEL::mCherry}$ suppressed the ER stress phenotype of *manf-1(tm3603)* mutants based on *hsp-4::GFP* analysis (Fig. 3 *A* and *B*).

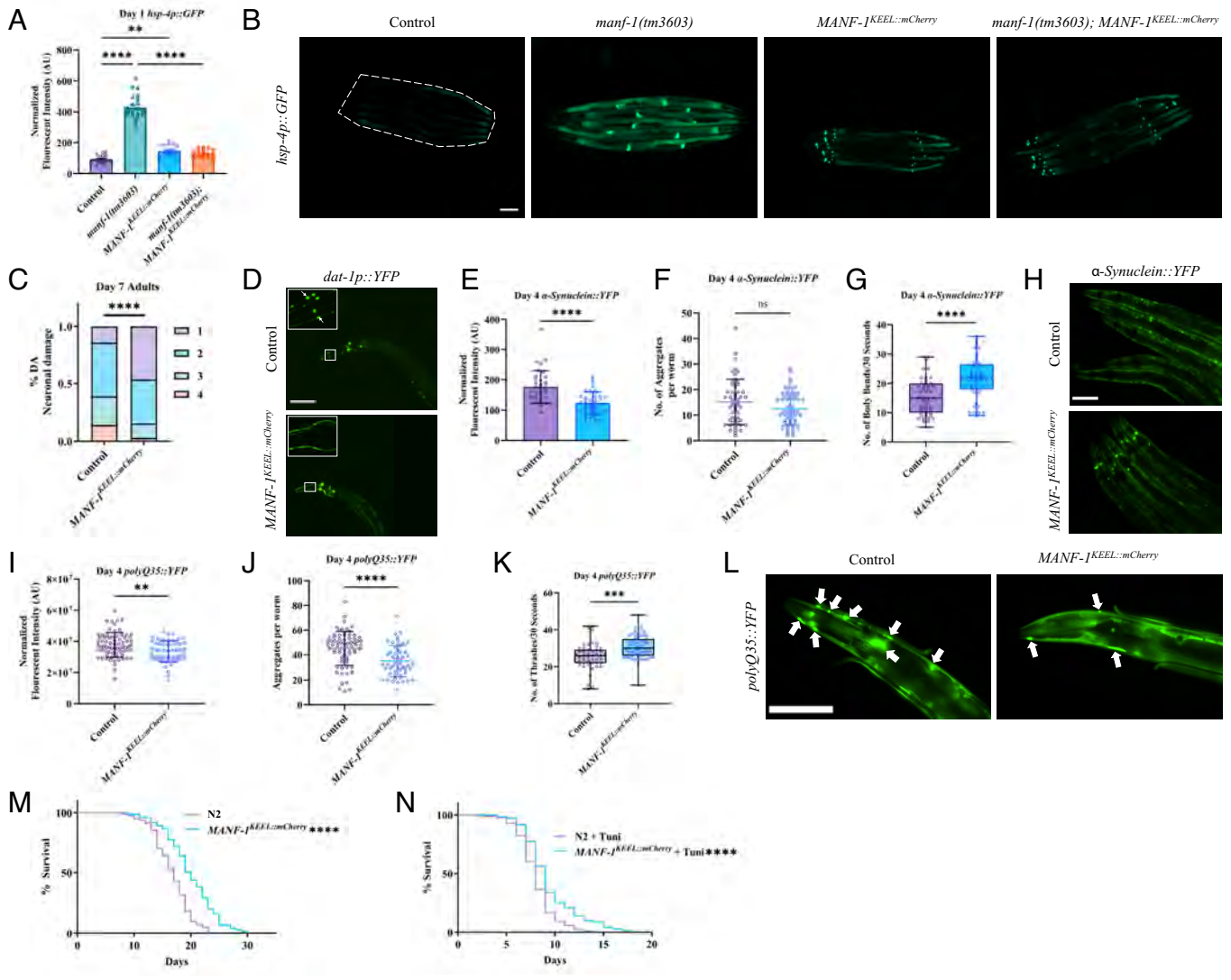

Fig. 3. MANF-1 overexpression rescues increased ER stress, protects DA neurons, reduces protein aggregation in disease models, and extends lifespan. (*A* and *B*) *hsp-4p::GFP* reporter expression in control, *manf-1(tm3603)*, *MANF-1*$^{KEEL::mCherry}$, and *manf-1(tm3603); MANF-1*$^{KEEL::mCherry}$ day 1 adults. Quantification of GFP fluorescence (*A*) and representative images (*B*). (Scale bar, 100 μm.) (*C* and *D*) Analysis of DA neurons in day 7 adults. (*C*) Neuronal defects were classified into four different categories. See Fig. 3 legend and *Materials and Methods* for details. (*D*) Corresponding images of DA neurons. (Scale bar, 100 μm.) Boxed regions show neurons at higher magnification. Arrows point to puncta in dendrites in the control worm. (*E–H*) The effect of *MANF-1*$^{KEEL::mCherry}$ on α-Synuclein::YFP aggregation in body wall muscles of day 4 adults. The panels show α-Synuclein::YFP fluorescence intensity (*E*), aggregates (*F*), thrashing response of animals (*G*), and representative images (*H*). (Scale bar, 100 μm.) (*I–L*) The effect of *MANF-1*$^{KEEL::mCherry}$ on polyQ35::YFP aggregation in body wall muscles of day 4 adults. Quantification of polyQ35::YFP fluorescence intensity (*I*) and protein aggregates (*J*). (*K*) Thrashing response over a 30-s interval. (*L*) Representative images of animals. (Scale bar, 100 μm.) Arrows mark aggregates in the head region. (*M* and *N*) Lifespan of wild-type N2 and *MANF-1*$^{KEEL::mCherry}$ animals without any treatment (*M*) and in the presence of 25 ng/μL tunicamycin (*N*). The mean and max lifespan are in Dataset S1. At least three batches with 10 to 30 worms per batch were examined for *A–L* and three batches with 20 to 30 animals per batch for *M* and *N*. Data in *A* are expressed as mean ± SEM and in *E–G*, *I*, and *J* as mean ± SD. Panels *G* and *K* show a box plot containing all data points along with the mean and 25th and 75th quartile boundaries. Data were analyzed using one-way ANOVA with Tukey's test (*A*), Chi-squared test (*C*), Student's *t* test (*E–G* and *I–K*), and log-rank (Kaplan–Meier) method (*M* and *N*). **P* < 0.05; ***P* < 0.01; ****P* < 0.001; *****P* < 0.0001.

To determine whether *MANF-1*$^{KEEL::mCherry}$ had protective capabilities, we examined the phenotypes of transgenic animals. *manf-1* overexpression caused less DA neurodegeneration compared to controls (Fig. 3 *C* and *D*). The analysis of protein aggregation phenotype revealed significantly reduced fluorescent intensity of α-Synuclein aggregation although the total aggregation count was unaffected (Fig. 3 *E*, *F*, and *H*). The animals also showed lower thrashing defect (Fig. 3*G*). Similarly, the polyQ defects were also reduced (Fig. 3 *I*–*L* and *SI Appendix*, Fig. S2*F*). To investigate whether decreased α-Synuclein::YFP and polyQ::YFP aggregates were due to lower amounts of chimeric proteins, we performed western blotting. The results revealed that levels of both proteins were comparable to controls (*SI Appendix*, Fig. S5), leading us to conclude that MANF-1 does not affect protein abundance but rather functions to inhibit protein aggregation.

Similar to *hsp::manf-1* animals, the *MANF-1*$^{KEEL::mCherry}$ animals had a significantly increased lifespan (19.2% higher; mean lifespan 19.9 ± 0.5 d compared with 16.7 ± 0.4 d for controls) (Fig. 3*M*). Furthermore, they showed higher resistance to chronic ER stress (Fig. 3*N*). The increase in lifespan was also observed in another independently generated *manf-1* overexpression strain (*manf-1p::manf-1*, termed *MANF-1*^{HAR}; mean lifespan 18.5 ± 0.9 d compared with 15.9 ± 0.5 d for controls) (*SI Appendix*, Fig. S7). Overall, these results demonstrate the multiple beneficial effects of MANF-1 in *C. elegans*.

MANF-1 Is Expressed Broadly, Secreted, and Localizes to Lysosomes Independent of the ER Retention Signal. Previously, we reported that *manf-1* is ubiquitously expressed in tissues such as the pharynx, hypodermis, and intestine (9, 10). To extend these findings to localization of secreted MANF, we altered the ER retention capability of MANF. For MANF to localize to the ER, the protein must have a signal peptide at the N terminus and a KDEL sequence (KEEL in worms) at the C terminus. We generated several new transgenic strains expressing MANF-1::mCherry chimeric proteins using an endogenous promoter (*SI Appendix*, Fig. S8). Two such strains contained either an obstructed or deleted retention signal with mCherry fused at the C terminus (*MANF-1*$^{KEEL::mCherry}$ and *MANF-1*$^{\Delta KEEL::mCherry}$, respectively); one carried an unobstructed and functional ER retention signal after mCherry (*MANF-1*$^{mCherry::KEEL}$), and the other one, a functional human version of the retention signal (*MANF-1*$^{mCherry::RTDL}$) (*SI Appendix*, Fig. S8). These different strains allowed us to investigate the subcellular localization of MANF-1 and how it might confer a protective response in animals.

The examination of *MANF-1*$^{KEEL::mCherry}$ and *MANF-1*$^{\Delta KEEL::mCherry}$ animals with putatively secreted MANF protein revealed that the chimeric protein was present throughout the body, including the hypodermis, pharynx, coelomocytes, and the extracellular space (Fig. 4 *A*–*F*′ and *SI Appendix*, Fig. S9 *A* and *B*). A detailed examination identified fluorescent vesicles in the hypodermal cells as lysosomes based on colocalization studies. Specifically, the MANF-1::mCherry pattern overlapped with the lysosomal dye, LysoTracker Green, and the lysosomal membrane marker *scav-3::GFP* (31) (Fig. 4 *G*, i–iii). Similar to the hypodermis, MANF-1 localization in coelomocytes was confirmed to be lysosomal by colocalization with another marker *lmp-1::GFP* (32) (Fig. 4 *G*, iv). These data provide evidence that MANF-1 is localized to the lysosomal membrane. The protein is secreted to the extracellular space which allows it to be taken up by other cells and coelomocytes.

An identical expression pattern was observed in two additional independently generated *MANF-1*$^{KEEL::mCherry}$ strains with lower amounts of *manf-1::mCherry* (*Materials and Methods*) (*SI Appendix*, Fig. S9 *A* and *B*). The MANF-1::mCherry positive structures in these and the *MANF-1*$^{\Delta KEEL::mCherry}$ strain were indistinguishable (*SI Appendix*, Fig. S9 *C* and *D*). Similar to *MANF-1*$^{KEEL::mCherry}$, *MANF-1*$^{\Delta KEEL::mCherry}$ animals showed significant lifespan extension and ER stress resistance (*SI Appendix*, Fig. S9 *E* and *F*). Another CRISPR-generated transgenic strain NK2548 (*manf-1p:: mKate2:: manf-1*) carrying *mKate2* reporter downstream of the endogenous *manf-1* signal sequence (10) also exhibited lysosomal localization of the chimeric protein upon treatment with tunicamycin (*SI Appendix*, Fig. S10*A*). Additionally, detailed examination of both the mKate2::MANF-1 and the previously existing *manf-1p::GFP* transcriptional line showed coelomocyte localization (*SI Appendix*, Fig. S10).

Further characterization of *manf-1* expression during aging revealed a dynamic pattern. As reported earlier for lysosomes (33), MANF-1::mCherry structures changed with age from a vesicular to tubular-like morphology (Fig. 4 *H* and *I*). No significant overlap was observed with MANS::GFP (golgi body) (32), *vha-6p::GFP::C34B2.10* (ER) (34), GFP::LGG-1 (autophagosomes) (35), mitoGFP (mitochondria) (36), and Bodipy 493/503 (lipid droplets) (*SI Appendix*, Fig. S11 *A*–*E*). Additionally, MANF-1::mCherry was not detected in the neurons based on the DA neuronal marker *dat-1p::YFP* and pan-neuronal marker *unc-119p::GFP* (37, 38) (*SI Appendix*, Fig. S11 *F* and *G*).

We also examined MANF-1::mCherry localization in *MANF-1*$^{mCherry::KEEL}$ and *MANF-1*$^{mCherry::RTDL}$ animals, both of which contain functional ER retention signal sequences (Fig. 5 *J*–*M* and *SI Appendix*, Fig. S12). The expression patterns of these strains were similar to the two secreted MANF strains, *MANF-1*$^{KEEL::mCherry}$ and *MANF-1*$^{\Delta KEEL::mCherry}$. In addition, we observed bright fluorescence in the intestine in a pattern resembling ER-like morphology, which is consistent with the role of *manf-1* in ER-UPR maintenance, and also in other tissues, such as the spermatheca and muscles (Fig. 4 *J*–*M* and *SI Appendix*, Fig. S12 *A* and *B*). Fluorescence was also observed in several neuron-like cells in the ventral cord. Intestinal and muscle expression was faint in early-stage larvae but became more prominent from the late larval stage and during adulthood. Both spermatheca were visible in adults and coincided with the egg-laying stage of the animals. Expression in lysosome-like structures became more prominent as the animals progressed from early larval to adult stages. *MANF-1*$^{mCherry::RTDL}$ animals exhibited a slightly more diffuse pattern of MANF-1::mCherry in the lysosomes (*SI Appendix*, Fig. S12 *C*–*I*).

Taken together, these data demonstrate that MANF-1 is broadly expressed and secreted. Its presence in various tissues is affected by both the native *C. elegans* and human versions of the ER retention signal. Intracellular MANF-1 localizes to lysosomes within hypodermal cells, where it may interact with other proteins to regulate lysosome function and proteostasis. These findings lead us to conclude that MANF-1 confers protective benefits on animals beyond its previously described role in the ER.

MANF-1 Affects Lysosome Formation and Expression of Lysosomal Genes. The expression pattern of *manf-1* along with the phenotypic studies of mutant and transgenic animals prompted us to use a transcriptomic approach to understand the changes in gene expression associated with various cellular and molecular processes. To this end, we examined the differentially expressed (DE) genes in *manf-1(tm3603)* and MANF-1^{HAR} animals. A comparison of down-regulated DE genes in *MANF-1*^{HAR} and up-regulated *in manf-1(tm3603)*, revealed 16 genes that were linked to terms such as ER function and ER-UPR maintenance (Fig. 5 *A* and *B* and Dataset S2). An inverse of this analysis, that is, genes up-regulated in MANF-1^{HAR} (5,943) with down-regulated genes in *manf-1(tm3603)* (776) identified an overlapping set of 388 genes that were enriched in various GO, KEGG, and WormCat terms including lysosome, lipid metabolism, metabolism, and other processes (Fig. 5 *C* and *D* and Dataset S2). The list consisted of proteases such as *cpr-6, asp-2, asp-5, asp-8,* and *asp-12*; the V-ATPase *vha-6*, and the ABC transporter *haf-9*.

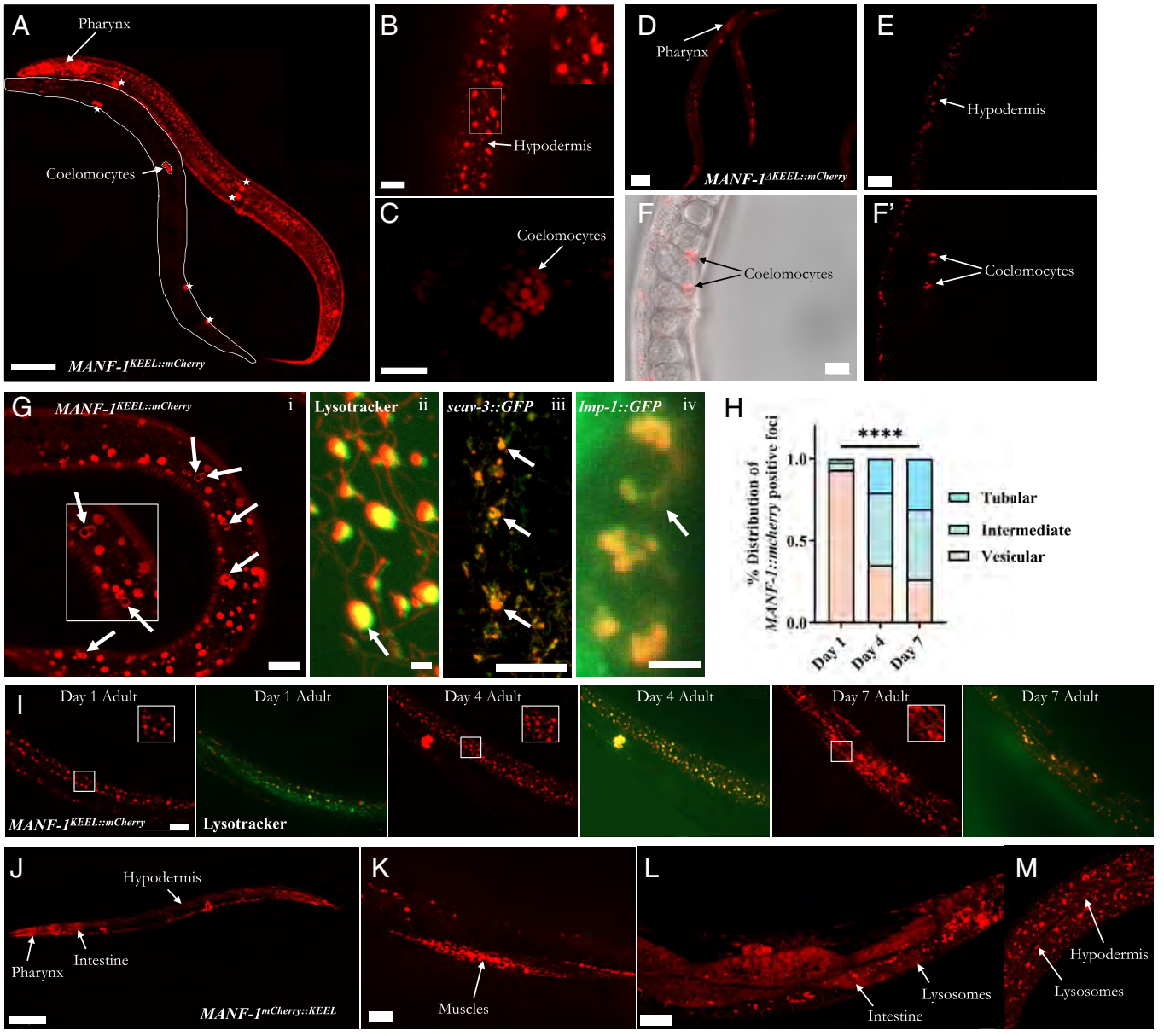

Fig. 4. MANF-1 expression analysis in *MANF-1*$^{KEEL::mCherry}$ animals showing lysosomal localization and age-related changes. (*A*) Two *MANF-1*$^{KEEL::mCherry}$ day 1 adults. The hypodermal region is in focus. The outlined worm has a weak fluorescence compared to the one next to it. Fluorescence is visible throughout the body including the pharynx and coelomocytes (arrows and stars). (Scale bar, 100 μm.) (*B* and *C*) Enlarged areas of animals showing fluorescence in hypodermal cells in clusters of varying sizes (Scale bar, 20 μm) (*B*) and in coelomocytes (Scale bar, 10 μm) (*C*). (*D–F'*) *MANF-1*$^{\Delta KEEL::mCherry}$ day 1 adult. Fluorescence is similar to the *MANF-1*$^{KEEL::mCherry}$ line and observed in the pharynx (Scale bar, 100 μm) (*D*), hypodermal cells (Scale bar, 20 μm) (*E*), and coelomocytes (Scale bar, 10 μm) (*F* and *F'*). (*G*, i–iv) Colocalization of MANF-1::mCherry and subcellular markers in hypodermal cells of day 1 adults. (*G*, i) A single confocal slice showing lysosomes. Arrows point to structures showing MANF-1 on the lysosomal membrane. (Scale bar, 10 μm.) (*G*, ii) MANF-1::mCherry colocalization with LysoTracker™ Green DND-26. (*G*, iii) Confocal image showing colocalization with SCAV-3::GFP. Arrows point to MANF-1 and SCAV-3 overlapping areas on lysosome membranes. (Scale bar, 20 μm.) (*G*, iv) Colocalization with LMP-1::GFP in coelomocytes. An arrow pointing to a ring structure showing overlapping fluorescence. (Scale bar, 5 μm.) (*H*) Quantification of MANF-1::mCherry fluorescing structures at different stages of adulthood. The foci were classified as vesicular, intermediate, or tubular and plotted as a stacked histogram. Worms were scored in at least three batches with 10 per batch. Data were analyzed using the Chi-squared test. *$P < 0.05$; **$P < 0.01$; ***$P < 0.001$; ****$P < 0.0001$. (*I*) *MANF-1*$^{KEEL::mCherry}$ animals at days 1, 4, and 7 of adulthood. (Scale bar, 20 μm.) Each animal was imaged for MANF-1::mCherry alone (red) and together with lysotracker (green). In all cases, hypodermal cells near the posterior region are shown. *Insets* show zoomed-in view of MANF-1::mCherry foci that change from vesicular to tubular-looking structures. (*J–M*) Confocal images of *MANF-1*$^{mCherry::KEEL}$ animals. (*J*) Fluorescence in this animal is visible in the pharynx, hypodermis, and one of the intestinal cells. (Scale bar, 100 μm.) (*K*) Zoomed-in view of a muscle fiber. (Scale bar, 20 μm.) An animal showing fluorescence in the intestinal (*L*) and hypodermal (*M*) regions. MANF-1::mCherry appears diffused with lysosomes appearing as bright fluorescing dots.

Following up on the transcriptomic results, we examined the lysosomes in *manf-1* null mutants. LysoTracker staining of *manf-1(tm3603)* animals revealed significantly fewer stained acidic organelles when compared with N2 and *MANF-1*$^{KEEL::mCherry}$ adults (Fig. 5 *E* and *F*). Another lysosomal marker *nuc-1::mCherry* (33) showed that lysosomes were smaller but present in a larger number in *manf-1* mutant worms (Fig. 5 *G–I*). There are several possibilities for differences in the LysoTracker and *nuc-1::mCherry* results. For example, *manf-1* mutants may have less efficient lysosomes regarding material uptake leading to *nuc-1::mCherry* expressing structures being smaller and with a reduced lysosomal storage capacity. Additionally, not all lysosomes may be acidic enough to stain efficiently with LysoTracker in *manf-1* mutants and with the lysosome size being smaller, would make it difficult to visualize them adequately. The lysosomal defect also included increased tubular morphology of *nuc-1::mCherry* in older adults (*SI Appendix*, Fig. S13).

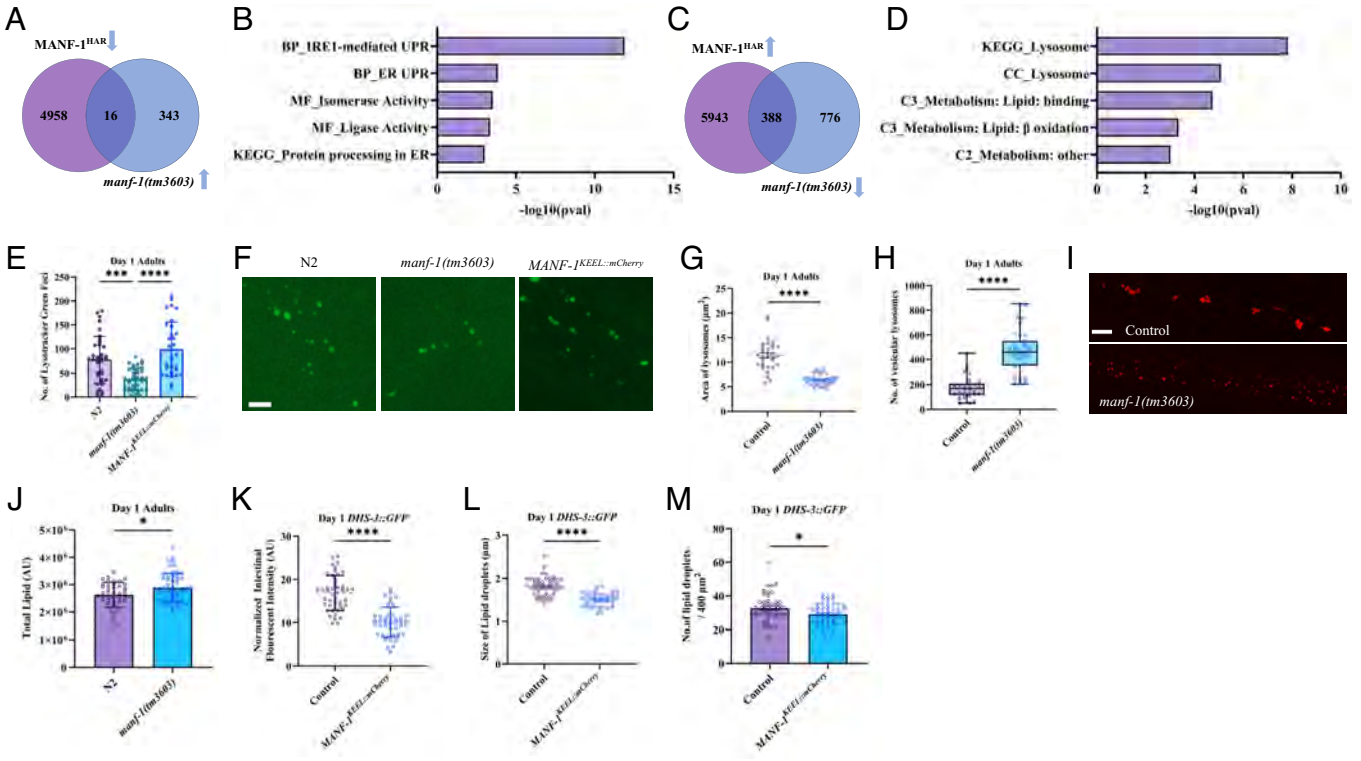

Fig. 5. Transcriptome profiling of *manf-1* mutant and overexpression strains and phenotypic analyses of animals showing changes in lysosomes and lipids. (*A* and *B*) An overlapping set of 16 genes that were down-regulated in MANF-1^{HAR} and up-regulated in *manf-1(tm3603)* animals. Venn diagram (*A*) and selected GO, KEGG, and WormCat categories generated using easyGSEA from the eVITTA toolbox (*B*). (*C* and *D*) An overlapping set of 388 genes that were up-regulated in MANF-1^{HAR} and down-regulated in *manf-1(tm3603)* animals. Data are plotted similar to panels *A* and *B*. (*E* and *F*) Lysotracker staining of N2, *manf-1(tm3603),* and *MANF-1$^{KEEL::mCherry}$* animals on day 1 of adulthood. Quantification of total lysosomes stained (*E*) and representative images (*F*). (Scale bar, 5 μm.) (*G–I*) Lysosome size and count based on the *nuc-1::mCherry* reporter in day 1 adults. Measurements of lysosomal area (*G*) and number (*H*) in the hypodermis. (*I*) Representative images corresponding to panels *G* and *H.* (Scale bar, 10 μm.) (*J*) Lipid quantification using Oil Red O staining. (*K–M*) Lipid quantification in the intestine using DHS-3::GFP. (*K*) Normalized GFP fluorescent intensity, (*L*) lipid droplets, and (*M*) number in a 400 μM^2 area. Animals were examined in at least three batches with (*E*, *G*, and *H*) 10 to 12 worms per batch and (*J–M*) 30 to 40 worms per batch. Data are expressed as mean ± SD (*E*, *J*, and *K*) and mean ± SEM (*G*, *L*, and *M*). Panel *H* shows a box plot containing all data points along with the mean and 25th and 75th quartile boundaries. Data were analyzed using one-way ANOVA with Tukey's test (*E*) and Student's *t* test (*G*, *H*, and *J–M*). *P < 0.05; **P < 0.01; ***P < 0.001; ****P < 0.0001.

As lysosomes regulate lipid metabolism and *manf-1* transcriptomes contained misregulated lipid-related genes (Dataset S2), we investigated whether lipid content was affected by the gene. The results showed that while *manf-1* mutants had more lipids, the phenotype was opposite in *MANF-1$^{KEEL::mCherry}$* animals (Fig. 5 *J–M* and *SI Appendix*, Fig. S14). Altogether, these data support the role of *manf-1* in lysosomal maintenance and its potential involvement in the autophagy lysosomal pathway.

MANF-1 Affects Autophagic Flux and Requires the Endosomal Pathway and HLH-30/TFEB for Its Function. Prompted by the MANF-1 expression pattern, mutant phenotype, and transcriptomic data, we analyzed the effect of *manf-1* on the autophagic process using two known factors LGG-1/LC3 and SQST-1/p62. While LGG-1 is involved in autophagosome formation, SQST-1 is an autophagy receptor that facilitates the degradation of ubiquitinated protein cargo (39, 40). The results showed that although the *lgg-1/LC3* and *sqst-1*/p62 transcripts were unaffected in *MANF-1$^{KEEL::mCherry}$* worms (Fig. 6*A*), a significant reduction was noted in GFP::LGG-1 and SQST-1::GFP fluorescent puncta (Fig. 6 *B–E*), consistent with increased autophagic clearance (41). In agreement with this, *manf-1(tm3603)* mutants exhibited an increased number of autophagosomes (Fig. 6 *B* and *C*).

We also used a tandem *mCherry::GFP::LGG-1* reporter to examine the effect of *manf-1* on autophagy. This reporter differentially marks autophagosomes (APs) and autolysosomes (ALs), such that APs emit both green (GFP) and red (mCherry) fluorescence whereas ALs emit only red fluorescence as the GFP signal is quenched (42). The results showed that *manf-1* RNAi caused a significant increase in APs compared to the control and a corresponding reduction in ALs (Fig. 6 *F* and *G*). These results suggest that in the absence of *manf-1*, autophagy is blocked and fewer APs fuse to lysosomes.

Next, we investigated the involvement of endosomal pathway components in mediating MANF-1's role in autophagy and its lysosomal localization. To this end, RAB-5 and RAB-7, two Rab GTPases affecting early and late trafficking, respectively, were examined. RNAi knockdown of *rab-7* resulted in *MANF-1$^{KEEL::mCherry}$* worms having the same amount of autophagosomes as controls, suggesting that autophagy was blocked (Fig. 6*H*). A similar phenotype was observed following *rab-5* RNAi (Fig. 6*I*), however the animals showed additional defects. Unlike control worms where MANF-1::mCherry fluorescence was present predominantly in vesicle-like structures, *rab-5* and *rab-7* RNAi caused a striking change in mCherry localization such that the fluorescence was significantly diffused (Fig. 6 *J* and *K*). We also observed that coelomocytes were much brighter in these animals. Additionally, abnormally large MANF-1::mCherry structures were present in hypodermal and seam cells, indicative of defects in MANF-1 transport (Fig. 6*L*). In some cases, GFP::LGG-1 fluorescence was overlapping with MANF-1::mCherry (Fig. 6*M*). Thus, endosomal components play an essential role in MANF-1 secretion and subcellular localization.

In addition to RNAi experiments, we studied the colocalization of MANF-1 with markers of the endosomal trafficking system. One of these, RME-8::GFP, localizes to endosomal membranes in coelomocytes and structures in hypodermal cells that may be cytoplasmic (43).

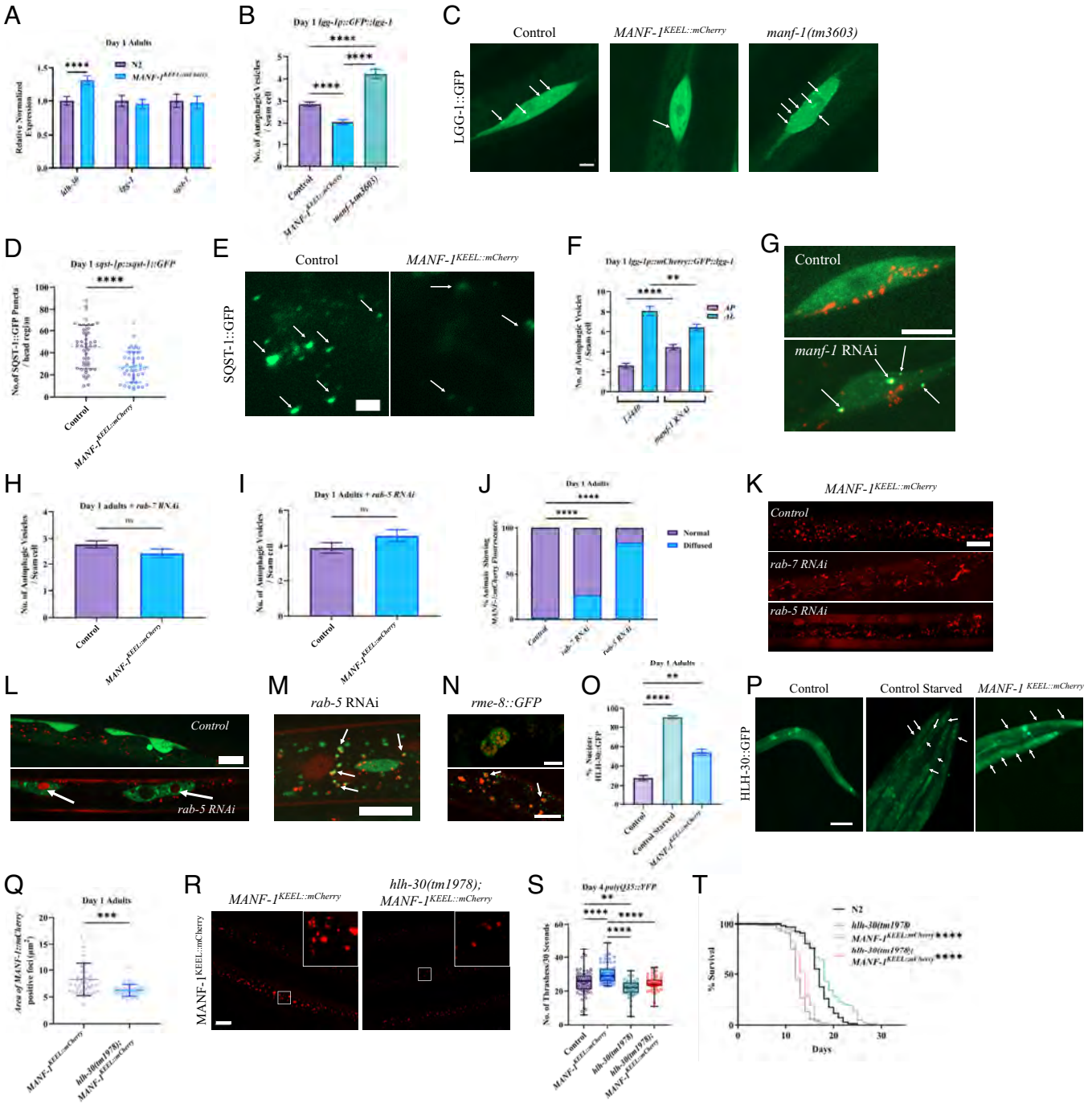

Fig. 6. MANF-1 utilizes endosomal trafficking to regulate autophagy and lysosome function in an HLH-30-dependent manner. (*A*) RT-qPCR analysis of *hlh-30, lgg-1,* and *sqst-1* transcripts. (*B*) Quantification of GFP::LGG-1 puncta in seam cells. (*C*) Representative images corresponding to panel *B*. Fluorescent puncta in GFP::LGG-1 seam cells are visible (arrows). (Scale bar, 5 μm.) (*D*) Quantification of SQST-1::GFP puncta in the head region. (*E*) Representative images corresponding to *D* showing the posterior pharyngeal bulb region. Arrows point to puncta in a 30 μm × 30 μm region. (Scale bar, 5 μm.) (*F*) Quantification of *lgg-1p::mCherry::GFP:lgg-1* tandem reporter in day 1 adults following *manf-1 RNAi*. (*G*) Representative images corresponding to panel *F*. Fluorescent structures represent autophagosomes (APs) carrying both mCherry and GFP and autolysosomes (ALs) with only mCherry. Arrows in the lower panel point to mCherry and GFP overlap in seam cells. (Scale bar, 10 μm.) (*H* and *I*) Quantification of GFP::LGG-1 puncta in seam cells following *rab-7* (*H*) and *rab-5* (*I*) *RNAi*. (*J*) Quantification of MANF-1::mCherry distribution. The distribution was classified as either normal or diffused and plotted as a stacked histogram. (*K*) Representative images showing fluorescing foci distribution corresponding to panel *J*. (Scale bar, 20 μm.) (*L*) Representative images showing defects in MANF-1::mCherry foci following *rab-5* RNAi. Arrows in the *Lower* panel point to abnormal structures in seam cells. The left arrow shows an abnormally large MANF-1::mCherry aggregate. The right arrow points to a hollow appearance. (Scale bar, 20 μm.) (*M*) Colocalization of MANF-1::mCherry with GFP::LGG-1 puncta (arrows) following *rab-5* RNAi. (Scale bar, 20 μm.) (*N*) No colocalization was observed with the endosome marker RME-8::GFP in coelomocytes (*Top* panel). Arrows point to cytoplasmic RME-8::GFP (*Bottom* panel) surrounding MANF-1::mCherry in the hypodermal region. (Scale bar, 10 μm.) (*O*) Quantification of nuclear HLH-30::GFP in *MANF-1*$^{KEEL::mCherry}$ day 1 adults. Wild-type and starved animals were used as negative and positive controls, respectively. The graph is plotted as cumulative percentage of animals with nuclear localization. (*P*) Representative images corresponding to (*O*). Arrows point to areas of intestinal nuclear localization. (Scale bar, 100 μm.) (*Q*) MANF-1::mCherry foci size in the hypodermis. (*R*) Representative images of MANF-1::mCherry foci corresponding to *Q*. (Scale bar, 20 μm.) (*S*) Thrashing rates of polyQ35::YFP expressing animals in a 30-s interval. (*T*) Lifespan analysis. Mean and max lifespan are in Dataset S1. (*A*) Three batches of pooled worms. (*B*, *D*, *O*, *Q*, *S*, and *T*) Three batches with 30 to 40 worms per batch were examined. (*F–J*) Three batches, with n = 10 to 15 worms per batch. Data are expressed as mean ± SEM (*A*, *B*, *F*, *H*, *I*, and *O*) and mean ± SD (*D* and *Q*). Panel *S* shows a box plot containing all data points along with the mean and 25th and 75th quartile boundaries. Data were analyzed using one-way ANOVA with Dunnett's test (*B* and *O*), Student's *t* test (*A*, *D*, *F*, *H*, *I*, and *Q*), Chi-squared test (*J*), one-way ANOVA with Tukey's test (*S*), and log-rank (Kaplan–Meier) method (*T*). **P* < 0.05; ***P* < 0.01; ****P* < 0.001; *****P* < 0.0001.

Our results showed that the cytoplasmic RME-8::GFP within the hypodermis appeared to surround MANF-1::mCherry fluorescence (Fig. 6*N*) While the colocalization of two proteins needs to be investigated in greater detail, these data together with Rab GTPase requirements lead us to conclude that MANF-1 utilizes the endo-lysosomal system for secretion and intracellular transport.

The unique role of MANF in lysosome function led us to question the mechanism by which MANF-1 may mediate its protective benefits. To this end, we searched the literature for proteins which play a major role in maintaining lysosome health and function. This led us to Transcription factor EB (TFEB), which is the major transcriptional regulator of lysosomal biogenesis and autophagy (44–47). TFEB controls various processes and is linked to diseases such as lysosomal storage disorders and neurodegeneration (48, 49). Under conditions that induce cellular stress, TFEB enters the nucleus to transcribe genes involved in autophagy and lysosome biogenesis. Additionally, TFEB overexpression or activation confers neuroprotection by clearing protein aggregates in neurodegenerative models (49). In *C. elegans*, HLH-30/TFEB has been shown to regulate lysosomal and autophagy genes and mediate the lifespan extension of long-lived animals (46, 47). We analyzed the HLH-30/TFEB pattern in *MANF-1*$^{KEEL::mCherry}$ animals and found the protein was predominantly localized to the nucleus (Fig. 6 *O* and *P*). As a positive control, starvation caused a significant increase in nuclear HLH-30/TFEB (Fig. 6 *O* and *P*). Additionally, *hlh-30* transcription was up-regulated following MANF-1 overexpression (Fig. 6*A*). Consistent with these results, *hlh-30(tm1978); MANF-1*$^{KEEL::mCherry}$ animals had smaller MANF-1::mCherry puncta compared to the controls (Fig. 6 *Q* and *R*). Thus, *hlh-30* has an essential role in mediating *manf-1* function, which is also supported by a slower thrashing rate (Fig. 6*S*) and shorter lifespan (Fig. 6*T*) of *MANF-1*$^{KEEL::mCherry}$ lacking *hlh-30* function. These results demonstrate that MANF-1 utilizes the HLH-30-mediated pathway to promote autophagy and lysosomal activity to promote proteostasis and longevity in animals.

Discussion

The neurotrophic factor MANF was initially identified for its role in promoting dopaminergic neuron survival but has since been found to affect various other processes (6, 21, 22, 50, 51). While much of the research on MANF has focused on its ER localization and regulation of ER-UPR, recent data suggest additional mechanisms of MANF function. Expression studies in animal models reveal MANF's cellular presence in many tissues and extracellular regions (12, 23, 25, 52, 53), highlighting its broad physiological significance.

Previous studies, including our own, have shown that *C. elegans* MANF-1 is crucial for protecting dopaminergic neurons from increased ER stress (9, 10, 25). In this study, we provide unique insights into MANF-1's role in stress response maintenance, proteostasis, and longevity. We found that *manf-1* mutants exhibit chronic ER-UPR activation and, when subjected to ER stress, show increased neurodegeneration and reduced lifespan. This is consistent with findings in other systems where both transcript and protein levels of MANF-1 increase in response to ER stress (13, 17, 54–56). Given that ER-UPR helps cells manage stress through enhanced protein folding and clearance of nonfunctional proteins (15, 57), we examined whether *manf-1* mutants have defects in these processes. Indeed, we observed increased protein aggregation in PD and HD models expressing human α-Synuclein and polyQ, respectively, particularly in older adults lacking *manf-1*, which resulted in abnormal locomotion and an age-dependent breakdown of proteostasis.

Our findings demonstrate that *manf-1* overexpression through different paradigms offers cytoprotective benefits, enhancing neuronal survival and promoting healthy aging. MANF-1 is expressed at various stages and in multiple cell types. Although MANF-1-expressing cells and DA neurons do not overlap significantly, neurons may be protected by the protein's extracellular uptake (25), as high levels of MANF-1::mCherry are observed in the pharynx and surrounding areas. Subcellular studies show MANF-1 predominantly in the intestine, pharynx, muscles, hypodermal cells, and coelomocytes, with similar patterns observed in strains carrying endogenous *manf-1p::mKate2::manf-1* and transcriptional *manf-1p::GFP* reporters. It is worth mentioning that our findings are supported by recent transcriptomic and proteomic studies (58, 59).

We found that MANF-1 expression was altered when the ER retention signal was blocked or deleted, resulting in weak or no localization of the protein in the intestine, muscles, and other areas, likely because it was secreted to the extracellular space. Previous cell culture studies showed that removing the ER retention sequence led to higher levels of MANF release into the culture media (13, 52). The shift in MANF-1::mCherry expression in transgenic animals lacking ER signals, combined with our results and rescue experiments, lead us to suggest that MANF-1 may be secreted from the intestinal ER and localizes to lysosomes in various cells to exert its cytoprotective function. Furthermore, the identification of the intestine as a likely synthesis point for MANF and the hypodermis as a target tissue for exported MANF opens broad avenues for exploring MANF's cell-non-autonomous function in vivo.

Our analysis of *C. elegans* MANF-1 was corroborated by transcriptomic data showing that lysosomal genes were repressed in mutant animals and activated in those overexpressing *manf-1*. A previous study in *D. melanogaster* also identified lysosomal genes that were down-regulated in MANF mutants (12). Additionally, the authors studied MANF localization in larvae, which revealed structures such as endosomes. Our work identified specific endosomal pathway components, i.e., RAB-5 and RAB-7 that are involved in MANF-1 transport in *C. elegans*. Overall, these findings suggest that MANF transport via the endosomal pathway and its role in lysosome function may be evolutionarily conserved.

Our study also provides evidence of MANF-1 expression in coelomocytes, scavenger cells crucial for material uptake from the pseudocoelom and endosomal to lysosomal trafficking (60). After uptake by coelomocytes, molecules travel through endocytic compartments and eventually enter lysosomes for degradation (61). Although the exact mechanism underlying MANF-1's role in coelomocytes remains unknown, it likely affects lysosomal function to maintain proteostasis. In support of this, a recent paper reported GO enrichment of lysosomal and endosomal terms in MANF-deficient macrophages (62). The authors also showed that recombinant MANF in older adults improved phagocytosis-induced lysosomal activity.

Emerging research has recognized lysosomes as cellular signaling hubs, with their dysregulation linked to various defects and neurodegenerative diseases (63, 64). The autophagy-lysosomal pathway is crucial for clearing toxic protein aggregates. We found that MANF-1$^{KEEL::mCherry}$ affects the gene expression and nuclear localization of HLH-30/TFEB, a transcriptional regulator of lysosomal and autophagy genes (49), essential for lifespan extension conferred by insulin/IGF-1 signaling and other longevity pathways (46). HLH-30 is essential for the lifespan and proteostasis benefits observed in MANF-1::mCherry animals. Previous studies showed that lysosomal calcium release can activate calcineurin to dephosphorylate TFEB, leading to its nuclear localization (49). Additionally,

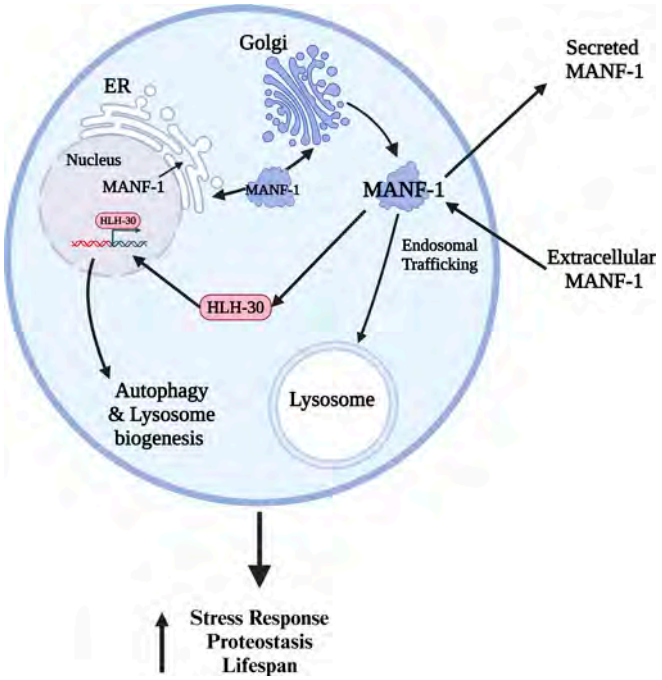

Fig. 7. A proposed model for MANF action. MANF-1 can be synthesized by cells or taken up from their extracellular environment. Within the cell, MANF-1 is retained in the ER through its native ER retention sequence and released in response to stress-inducing conditions. Once released from the ER, MANF-1 localizes to lysosomes as well as secreted out. The intracellular transport and secretion are mediated by the endosomal trafficking. The cytoprotective benefits of MANF-1 depend on the HLH-30-mediated signaling. Image created with BioRender.com.

lysosomal calcium can trigger ER calcium release and signaling (49, 63). These observations, coupled with data showing that ER calcium changes promote MANF secretion (13), support a model where MANF is part of a network that facilitates ER and lysosome cross talk to regulate TFEB-mediated activation of autophagy and proteostasis (Fig. 7). Notably, we observed a reduction in MANF-1-positive foci in *hlh-30* mutants, raising the possibility of a feedback mechanism. In support of this, the *manf-1* promoter contains sequences overlapping with the HLH-30 CLEAR-binding motif (www.wormbase.org) (45). Thus, similar to the lysosomal gene targets of TFEB (46), it is conceivable that *manf-1* is transcriptionally regulated by *hlh-30* and forms a positive regulatory network.

Given MANF-1's role in lysosome-mediated signaling and HLH-30/TFEB's involvement, we investigated LGG-1/Atg8/LC3 and SQST-1/p62 function in mediating autophagy (40, 65–68). An increase in LGG-1 and SQST-1 puncta may indicate autophagy blockage, while a reduction in both types of puncta implies increased autophagic flux. We found that MANF-1$^{KEEL::mCherry}$ animals exhibited reduced GFP::LGG-1 and SQST-1::GFP puncta, suggesting that MANF-1 promotes autophagy. Conversely, *manf-1(tm3603)* animals showed increased GFP::LGG-1 puncta. A double fluorescent reporter strain, *mCherry::GFP::LGG-1*, was also used which showed an increase in autophagosomes with a concomitant decrease in autolysosomes. Consistent with our findings, a recent study reported that MANF overexpression in mouse kidney cells promoted autophagy and mitochondrial biogenesis (41), observing a decrease in p62 abundance and finding that p-AMPK and FOXO3 play roles in promoting mitochondrial biogenesis. However, whether *C. elegans* AAK-2/AMPK and DAF-16/FOXO are involved in MANF-1-mediated processes requires further investigation.

Our findings on HLH-30-mediated MANF-1 function were supported by lipid analysis. As ER-UPR, autophagy, and lysosomes affect lipid metabolism (69–71), and *manf-1* transcriptomes identified lipid-related genes, we examined neutral lipids in *manf-1* mutants and found significantly higher levels. As expected, *MANF-1*$^{KEEL::mCherry}$ animals exhibited the opposite phenotype, with reduced number and size of lipid droplets. Previously, TFEB was shown to be necessary for lipid droplet clearance and lipid catabolism (49); in relation to this, mammalian TFEB and worm HLH-30 were found to regulate lysosomal genes and the fusion of lipid droplets to lysosomes in a process called lipophagy (47, 72). These data underscore the importance of MANF-1-HLH-30 signaling in multiple lysosome-mediated processes.

The presence of MANF-1 on lysosomes and its interactions with HLH-30 to mediate proteostasis raise various questions. How does MANF-1 reach lysosomes, and how does it cause HLH-30 to translocate to the nucleus? First, MANF-1 must be secreted from the ER to be cytoprotective. One possibility is that MANF-1 traffics through the Golgi to enter the endo-lysosomal pathway, reaching lysosomes. Once in this pathway, MANF-1 may enhance autophagic flux through improved lysosome function. This model is supported by *manf-1* RNAi blocking autophagy and reducing lysosome numbers, impacting overall animal health. MANF-1 may also follow the endosomal pathway to lysosomes, where it may interact with other membrane proteins. It would be interesting to investigate whether MANF-1 affects the calcium channel MCOLN1 to release lysosomal calcium into the cytoplasm and/or interacts with MTOR components to cause HLH-30's nuclear localization (49, 63). Further experiments are needed to explore these possibilities. Lysosome dysfunction due to changes in the cellular environment is known to trigger TFEB dephosphorylation, causing its nuclear localization (49). It is plausible that MANF-1 regulates HLH-30 by facilitating its dephosphorylation directly or indirectly, allowing nuclear entry. Mammalian MANF is an ATP binding protein that serves as a cofactor of GRP78 (17). Whether a similar interaction occurs between MANF-1 and HLH-30, that affects HLH-30 localization and in turn results in changes in MANF-1 expression in a feedback manner remains to be seen.

Our results have broad implications for understanding MANF function in higher eukaryotes and manipulating its role in promoting healthy aging and treating diseases, including lysosomal disorders. In this regard, it is worth noting that *manf* expression is down-regulated in Niemann-Pick and Gaucher disease models (73, 74). Future work will help elucidate the precise mechanisms of MANF localization, HLH-30/TFEB interaction, and stress response signaling that collectively promote neuronal health, proteostasis maintenance, and longevity.

Materials and Methods

Strains were cultured on standard NGM (nematode growth media) agar plates using established protocols. Plates were seeded with *Escherichia coli* bacterial strain OP50 as a food source (75). Worms were grown and maintained at 20 °C unless stated otherwise. N2 was used as a wild-type control.

The strains used in this study are listed in Dataset S3. Detailed methods are provided in *SI Appendix, Supplementary Materials and Methods*.

Data, Materials, and Software Availability. All study data are included in the article and/or supporting information.

ACKNOWLEDGMENTS. This work was supported by the Natural Sciences and Engineering Research Council of Canada Discovery grant to B.P.G. and partially supported by the NIH (R00-ES029552 to J.H.H.). Some of the strains were obtained from the *Caenorhabditis* Genetics Center, which is funded by the NIH Office of Research Infrastructure Programs (P40 OD010440). The pGLC130 plasmid was made by Komal Prajapati. We thank WormBase for its citation

database on individual genes (PMID 19910365) and the McMaster biology department confocal resource for assistance with imaging. Ram Mishra and Ravi Selvaganapathy provided feedback on some of the experiments. We thank Dr. Kacy Gordon (University of North Carolina–Chapel Hill) for her assistance with generating the MANF-1^{HAR} overexpression line.

Author affiliations: [a]Department of Biology, McMaster University, Hamilton, ON L8S 4K1, Canada; [b]Department of Biochemistry and Molecular Biology, Medical University of South Carolina, Charleston, SC 29425; and [c]Department of Regenerative Medicine and Cell Biology, Medical University of South Carolina, Charleston, SC 29425

Author contributions: B.P.G. and S.K.B.T. designed research; S.K.B.T. and J.H.H. performed research; S.K.B.T. and J.H.H. contributed new reagents/analytic tools; S.K.B.T., J.H.H., and B.P.G. analyzed data; and S.K.B.T. and B.P.G. wrote the paper.

1. R. C. Taylor, A. Dillin, Aging as an event of proteostasis collapse. *Cold Spring Harb. Perspect. Biol.* **3**, a004440 (2011).
2. R. C. Taylor, C. Hetz, Mastering organismal aging through the endoplasmic reticulum proteostasis network. *Aging Cell* **19**, e13265 (2020).
3. J. Labbadia, R. I. Morimoto, The biology of proteostasis in aging and disease. *Annu. Rev. Biochem.* **84**, 435–464 (2015).
4. C. Hetz, S. Saxena, ER stress and the unfolded protein response in neurodegeneration. *Nat. Rev. Neurol.* **13**, 477–491 (2017).
5. P. Remondelli, M. Renna, The endoplasmic reticulum unfolded protein response in neurodegenerative disorders and its potential therapeutic significance. *Front. Mol. Neurosci.* **10**, 187 (2017).
6. A. Nasrolahi *et al.*, Neurotrophic factors hold promise for the future of Parkinson's disease treatment: Is there a light at the end of the tunnel? *Rev. Neurosci.* **29**, 475–489 (2018).
7. E. Pakarinen, P. Lindholm, CDNF and MANF in the brain dopamine system and their potential as treatment for Parkinson's disease. *Front. Psychiatry* **14**, 1188697 (2023).
8. M. Lindahl, M. Saarma, P. Lindholm, Unconventional neurotrophic factors CDNF and MANF: Structure, physiological functions and therapeutic potential. *Neurobiol. Dis.* **97**, 90–102 (2017).
9. C. Richman *et al.*, *C. elegans* MANF homolog is necessary for the protection of dopaminergic neurons and ER unfolded protein response. *Front. Neurosci.* **12**, 544 (2018).
10. J. H. Hartman *et al.*, MANF deletion abrogates early larval *Caenorhabditis elegans* stress response to tunicamycin and *Pseudomonas aeruginosa*. *Eur. J. Cell Biol.* **98**, 151043 (2019).
11. M. H. Voutilainen *et al.*, Therapeutic potential of the endoplasmic reticulum located and secreted CDNF/MANF family of neurotrophic factors in Parkinson's disease. *FEBS Lett.* **589**, 3739–3748 (2015).
12. M. Palgi *et al.*, Gene expression analysis of *Drosophila* Manf mutants reveals perturbations in membrane traffic and major metabolic changes. *BMC Genomics* **13**, 134 (2012).
13. C. C. Glembotski *et al.*, Mesencephalic astrocyte-derived neurotrophic factor protects the heart from ischemic damage and is selectively secreted upon sarco/endoplasmic reticulum calcium depletion. *J. Biol. Chem.* **287**, 25893–25904 (2012).
14. Y. C. Chen *et al.*, MANF regulates dopaminergic neuron development in larval zebrafish. *Dev. Biol.* **370**, 237–249 (2012).
15. P. Walter, D. Ron, The unfolded protein response: From stress pathway to homeostatic regulation. *Science* **334**, 1081–1086 (2011).
16. G. Mercado, P. Valdes, C. Hetz, An ERcentric view of Parkinson's disease. *Trends Mol. Med.* **19**, 165–175 (2013).
17. A. Eesmaa *et al.*, The cytoprotective protein MANF promotes neuronal survival independently from its role as a GRP78 cofactor. *J. Biol. Chem.* **296**, 100295 (2021).
18. V. Kovaleva *et al.*, MANF regulates neuronal survival and UPR through its ER-located receptor IRE1alpha. *Cell Rep.* **42**, 112066 (2023).
19. H. Lohelaid *et al.*, UPR responsive genes Manf and Xbp1 in stroke. *Front. Cell Neurosci.* **16**, 900725 (2022).
20. M. Jäntti, B. K. Harvey, Trophic activities of endoplasmic reticulum proteins CDNF and MANF. *Cell Tissue Res.* **382**, 83–100 (2020).
21. J. Neves *et al.*, Immune modulation by MANF promotes tissue repair and regenerative success in the retina. *Science* **353**, aaf3646 (2016).
22. P. Sousa-Victor *et al.*, MANF regulates metabolic and immune homeostasis in ageing and protects against liver damage. *Nat. Metab.* **1**, 276–290 (2019).
23. T. Danilova *et al.*, Mesencephalic astrocyte-derived neurotrophic factor (MANF) is highly expressed in mouse tissues with metabolic function. *Front. Endocrinol. (Lausanne)* **10**, 765 (2019).
24. M. Peled *et al.*, Mesencephalic astrocyte-derived neurotrophic factor is secreted from interferon-gamma-activated tumor cells through ER calcium depletion. *PLoS ONE* **16**, e0250178 (2021).
25. M. Bai *et al.*, Conserved roles of *C. elegans* and human MANFs in sulfatide binding and cytoprotection. *Nat. Commun.* **9**, 897 (2018).
26. Z. Zhang *et al.*, MANF protects dopamine neurons and locomotion defects from a human alpha-synuclein induced Parkinson's disease model in *C. elegans* by regulating ER stress and autophagy pathways. *Exp. Neurol.* **308**, 59–71 (2018).
27. R. C. Taylor, A. Dillin, XBP-1 is a cell-nonautonomous regulator of stress resistance and longevity. *Cell* **153**, 1435–1447 (2013).
28. J. F. Morley *et al.*, The threshold for polyglutamine-expansion protein aggregation and cellular toxicity is dynamic and influenced by aging in *Caenorhabditis elegans*. *Proc. Natl. Acad. Sci. U.S.A.* **99**, 10417–10422 (2002).
29. F. A. Abu-Hijleh *et al.*, Novel mechanism of action for the mood stabilizer lithium. *Bipolar Disord.* **23**, 76–83 (2021).
30. K. Nawar, "MANF, ER stress and the pathophysiology of Parkinson's disease", MSc thesis, McMaster University, Hamilton, ON, Canada (2019).
31. Y. Li *et al.*, The lysosomal membrane protein SCAV-3 maintains lysosome integrity and adult longevity. *J. Cell Biol.* **215**, 167–185 (2016).
32. S. Treusch *et al.*, *Caenorhabditis elegans* functional orthologue of human protein h-mucolipin-1 is required for lysosome biogenesis. *Proc. Natl. Acad. Sci. U.S.A.* **101**, 4483–4488 (2004).
33. Y. Sun *et al.*, Lysosome activity is modulated by multiple longevity pathways and is important for lifespan extension in *C. elegans*. *eLife* **9**, e55745 (2020).
34. N. Xu *et al.*, The FATP1-DGAT2 complex facilitates lipid droplet expansion at the ER-lipid droplet interface. *J. Cell Biol.* **198**, 895–911 (2012).
35. L. R. Lapierre *et al.*, Autophagy and lipid metabolism coordinately modulate life span in germline-less *C. elegans*. *Curr. Biol.* **21**, 1507–1514 (2011).
36. A. M. Labrousse *et al.*, *C. elegans* dynamin-related protein DRP-1 controls severing of the mitochondrial outer membrane. *Mol. Cell* **4**, 815–826 (1999).
37. R. Nass *et al.*, Neurotoxin-induced degeneration of dopamine neurons in *Caenorhabditis elegans*. *Proc. Natl. Acad. Sci. U.S.A.* **99**, 3264–3269 (2002).
38. M. Maduro, D. Pilgrim, Identification and cloning of unc-119, a gene expressed in the *Caenorhabditis elegans* nervous system. *Genetics* **141**, 977–988 (1995).
39. C. Kumsta *et al.*, The autophagy receptor p62/SQST-1 promotes proteostasis and longevity in *C. elegans* by inducing autophagy. *Nat. Commun.* **10**, 5648 (2019).
40. C. Ploumi, A. Sotiriou, N. Tavernarakis, Monitoring autophagic flux in *Caenorhabditis elegans* using a p62/SQST-1 reporter. *Methods Cell Biol.* **165**, 73–87 (2021).
41. Y. Kim *et al.*, MANF stimulates autophagy and restores mitochondrial homeostasis to treat autosomal dominant tubulointerstitial kidney disease in mice. *Nat. Commun.* **14**, 6493 (2023).
42. J. T. Chang *et al.*, Spatiotemporal regulation of autophagy during *Caenorhabditis elegans* aging. *eLife* **6**, e18459 (2017).
43. Y. Zhang, B. Grant, D. Hirsh, RME-8, a conserved J-domain protein, is required for endocytosis in *Caenorhabditis elegans*. *Mol. Biol. Cell* **12**, 2011–2021 (2001).
44. C. Settembre *et al.*, TFEB links autophagy to lysosomal biogenesis. *Science* **332**, 1429–1433 (2011).
45. M. Sardiello *et al.*, A gene network regulating lysosomal biogenesis and function. *Science* **325**, 473–477 (2009).
46. L. R. Lapierre *et al.*, The TFEB orthologue HLH-30 regulates autophagy and modulates longevity in *Caenorhabditis elegans*. *Nat. Commun.* **4**, 2267 (2013).
47. E. J. O'Rourke, G. Ruvkun, MXL-3 and HLH-30 transcriptionally link lipolysis and autophagy to nutrient availability. *Nat. Cell Biol.* **15**, 668–676 (2013).
48. A. Tan *et al.*, Past, present, and future perspectives of transcription factor EB (TFEB): Mechanisms of regulation and association with disease. *Cell Death Differ.* **29**, 1433–1449 (2022).
49. G. Napolitano, A. Ballabio, TFEB at a glance. *J. Cell Sci.* **129**, 2475–2481 (2016).
50. P. Petrova *et al.*, MANF: A new mesencephalic, astrocyte-derived neurotrophic factor with selectivity for dopaminergic neurons. *J. Mol. Neurosci.* **20**, 173–188 (2003).
51. M. H. Voutilainen *et al.*, Mesencephalic astrocyte-derived neurotrophic factor is neurorestorative in rat model of Parkinson's disease. *J. Neurosci.* **29**, 9651–9659 (2009).
52. M. J. Henderson *et al.*, Mesencephalic astrocyte-derived neurotrophic factor (MANF) secretion and cell surface binding are modulated by KDEL receptors. *J. Biol. Chem.* **288**, 4209–4225 (2013).
53. P. Lindholm *et al.*, MANF is widely expressed in mammalian tissues and differently regulated after ischemic and epileptic insults in rodent brain. *Mol. Cell. Neurosci.* **39**, 356–371 (2008).
54. R. Lindstrom *et al.*, Exploring the conserved role of MANF in the unfolded protein response in *Drosophila melanogaster*. *PLoS ONE* **11**, e0151550 (2016).
55. A. Tadimalla *et al.*, Mesencephalic astrocyte-derived neurotrophic factor is an ischemia-inducible secreted endoplasmic reticulum stress response protein in the heart. *Circ. Res.* **103**, 1249–1258 (2008).
56. S. Xu *et al.*, Mesencephalic astrocyte-derived neurotrophic factor (MANF) protects against Abeta toxicity via attenuating Abeta-induced endoplasmic reticulum stress. *J. Neuroinflamm.* **16**, 35 (2019).
57. C. Hetz, E. Chevet, H. P. Harding, Targeting the unfolded protein response in disease. *Nat. Rev. Drug Discov.* **12**, 703–719 (2013).
58. C.-H. Tan *et al.*, Single tissue proteomics in *Caenorhabditis elegans* reveals proteins resident in intestinal lysosome-related organelles. *Proc. Natl. Acad. Sci. U.S.A.* **121**, e2322588121 (2024).
59. A. L. Schorr *et al.*, An updated *C. elegans* nuclear body muscle transcriptome for studies in muscle formation and function. *Skelet. Muscle* **13**, 4 (2023).
60. H. Fares, I. Greenwald, Genetic analysis of endocytosis in *Caenorhabditis elegans*: Coelomocyte uptake defective mutants. *Genetics* **159**, 133–145 (2001).
61. K. Gee *et al.*, Regulators of lysosome function and dynamics in *Caenorhabditis elegans*. *G3 (Bethesda)* **7**, 991–1000 (2017).
62. N. S. Sousa *et al.*, Aging disrupts MANF-mediated immune modulation during skeletal muscle regeneration. *Nat. Aging* **3**, 585–599 (2023).
63. S. R. Bonam, F. Wang, S. Muller, Lysosomes as a therapeutic target. *Nat. Rev. Drug Discov.* **18**, 923–948 (2019).
64. R. E. Lawrence, R. Zoncu, The lysosome as a cellular centre for signalling, metabolism and quality control. *Nat. Cell Biol.* **21**, 133–142 (2019).
65. S. Henis-Korenblit, A. Melendez, Methods to determine the role of autophagy proteins in *C. elegans* aging. *Methods Mol. Biol.* **1880**, 561–586 (2019).
66. N. J. Palmisano, A. Melendez, Detection of autophagy in *Caenorhabditis elegans*. *Cold Spring Harb. Protoc.* 2016, pdb.prot086496 (2016).
67. N. J. Palmisano, A. Melendez, Detection of autophagy in *Caenorhabditis elegans* using GFP::LGG-1 as an autophagy marker. *Cold Spring Harb. Protoc.* **2016**, pdb.prot086496 (2016).
68. C. Ploumi, E. Kyriakakis, N. Tavernarakis, Coupling of autophagy and the mitochondrial intrinsic apoptosis pathway modulates proteostasis and ageing in *Caenorhabditis elegans*. *Cell Death Dis.* **14**, 110 (2023).
69. M. Moncan *et al.*, Regulation of lipid metabolism by the unfolded protein response. *J. Cell Mol. Med.* **25**, 1359–1370 (2021).
70. R. Singh *et al.*, Autophagy regulates lipid metabolism. *Nature* **458**, 1131–1135 (2009).
71. J. Xu, S. Taubert, Beyond proteostasis: Lipid metabolism as a new player in ER homeostasis. *Metabolites* **11**, 52 (2021).
72. C. Settembre *et al.*, TFEB controls cellular lipid metabolism through a starvation-induced autoregulatory loop. *Nat. Cell Biol.* **15**, 647–658 (2013).
73. A. Cougnoux *et al.*, Single cell transcriptome analysis of Niemann–Pick disease, type C1 cerebella. *Int. J. Mol. Sci.* **21**, 5368 (2020).
74. N. Dasgupta *et al.*, Gaucher disease: Transcriptome analyses using microarray or mRNA sequencing in a Gba1 mutant mouse model treated with velaglucerase alfa or imiglucerase. *PLoS ONE* **8**, e74912 (2013).
75. S. Brenner, The genetics of *Caenorhabditis elegans*. *Genetics* **77**, 71–94 (1974).